J. Electrochem. Sci. Eng. **00(0)** (2023) 000-000; http://dx.doi.org/10.5599/jese.1697

Open Access : : ISSN 1847-9286
www.jESE-online.org

Original scientific paper

The performance of heteroatom-doped carbon nanotubes synthesized *via* a hydrothermal method on the oxygen reduction reaction and specific capacitance

Tienah H. H. Elagib[1,2,✉], Nassereldeen A. Kabbashi[1], Md Zahangir Alam[1], Ma'an F. Al-Khatib[1], Mohamed E. S. Mirghani[1] and Elwathig A. M. Hassan[2]

[1]*Kulliyyah of Engineering, Department of Chemical Engineering and Sustainability, International Islamic University Malaysia, Jalan Gombak 53100, Kuala Lumpur, Malaysia*
[2]*Department of Materials Engineering, Faculty of Industrial Engineering and Technology, University of Gezira, Wad Madani, Sudan*

Corresponding author: ✉tienahhussain25024@gmail.com

Received: February 7, 2023; Accepted: April 16, 2023; Published: May xx, 2023

Abstract

Due to the increasing demand for electrochemical energy storage, various novel electrode and catalysis materials for supercapacitors and rechargeable batteries have developed over the last decade. The structure and characteristics of these catalyst materials have a major effect on the device's performance. In order to lower the costs associated with electrochemical systems, electrochemical systems, metal-free catalysis materials can be employed. In this study, metal-free catalysts composed of nitrogen (N) and sulfur (S) dual-doped multi-walled carbon nanotubes were synthesized using a straightforward and cost-effective single-step hydrothermal method. Carbon nanotubes served as the carbon source, while l-cysteine amino acid and thiourea acted as doping elements. As a result of the physicochemical characterization, many defects and a porous structure were noted, along with the successful insertion of nitrogen and sulfur into the carbon nanotube was confirmed. According to the cyclic voltammetry tests for the dual-doped samples in alkaline conditions, the D-CNT2 catalyst exhibited onset potentials of -0.30 V higher than the -0.37 V observed for the D-CNT3 catalyst. This indicates enhanced oxygen–reduction reaction due to the synergistic effects of the heteroatoms in the structure and the presence of chemically active sites. Moreover, the outstanding specific capacitance of the D-CNT2 catalyst (214.12 F g^{-1} at scanning rates of 1 mV s^{-1}) reflects the effective porosity of the proposed catalyst. These findings highlight the potential of N/S dual–doped carbon nanotubes for electrocatalytic applications, contributing to efficient energy conversion.

Keywords

Metal-free catalyst; electrochemical energy storage; catalytic activity; porous structure

Introduction

In recent years, fostering a sustainable society has been a focus [1-3]. Developing renewable energy is important in achieving sustainable development and reducing pollution from fossil fuels [4-6]. The creation of clean energy storage and generation with low costs and great efficiency has garnered a lot of interest [7-9]. Traditional energy supplies, according to the Exxon Mobil paper titled 2018 Outlook for Energy: a view of 2040, will play an irreplaceable part in our future daily lives. Despite efficiency increases between 2016 and 2040, it expected worldwide energy consumption to increase by approximately 25 %, while they expected global electricity demand to climb by 60 %. Thus, building green electro-based energy systems is urgently needed to support economic progress and accomplish the Paris Agreement's climate targets, and it surely bears enormous market opportunities [10].

Presently, vital research is being focused on advanced technologies for electrochemical energy storage and conversion systems such as electrochemical capacitors, regenerative fuel cells, and rechargeable batteries (including Na-ion batteries, Li–sulfur batteries, Li-ion batteries, and K-ion batteries [11]), including electrocatalysis due to their flexible capacities [12], eco-friendly [13-15], remarkable energy conversion ability, and sustainability [16,17]. Electrochemical processes, like electrocatalysis, are crucial to electrochemical energy storage and conversion systems [18]. During discharging, such energy systems undergo an oxygen reduction reaction (ORR) on their negative electrode [19]. It is important to rationally design highly active [20], durable, and low-cost electrocatalyst for effective ORR as it represents a critical reaction in energy conversion systems [21]. Although a variety of factors influence the performance of energy-related devices, the structure and characteristics of the materials utilized heavily influence the overall performance [22].

In fact, ORR is slow in an acidic medium and requires noble catalysts such as Pt to occur; however, ORR has a lower over-potential in an alkaline medium than that in an acidic medium, allowing the use of noble-free catalysts [23]. To meet the needs of industry and advanced energy systems, the advancement of cost-effective metal-free electrocatalytic materials is of great interest [24]. In this direction, numerous non-precious ORR electrocatalysts, such as transition metal chalcogenides [25], transition metal nitrogen-containing complexes, and metal-free doped carbon materials [26], have been explored and developed [27]. It is broadly acknowledged that doping nanostructured carbons with heteroatoms such as boron, nitrogen (N), phosphorus, and sulfur (S) improves oxygen-reaction activities significantly [28]. For instance, J. H. Kim *et al.* [29] used chemical vapor deposition to create sulfur-doped carbon nanotubes (S-CNTs) using dimethyl disulfide as the sulfur source. At a high discharge current density of 100 mA cm^{-2}, the proposed material exhibited excellent specific capacitance of 120.2 F g^{-1}. The doping effect was responsible for the superior electrochemical performance of S-CNTs. As earlier reported in the literature, the doped heteroatoms can modify the spin-charge densities, causing charge redistribution in the carbon matrix [30]. The S element, in particular, increases the positive charge density and spin density of adjacent carbon atoms, promoting oxygen molecular adsorption on the carbon matrix and conferring carbon materials with effective ORR catalytic activity [31,32]. The creation of C-N structures, such as graphitic-N and pyridinic-N, can aid in electron transfer during the ORR process [31]. Previous research has shown that incorporating heteroatoms improves the distribution and preserves the electrical conductivity of nanostructured carbons and, thus, catalytic activity. The doped material also has long-term durability, good stability [33], and exceptional poison resistance during the ORR process [34,35]. Raji Atchudan and co-workers [36], for example, synthesized nitrogen-doped porous carbon, which showed a high specific capacity (160 F g^{-1}) with a good cycling stability of 95 % and a high rate performance of 52 % retention from 0.5 to 5.0 A g^{-1} in a three-electrode system in an aqueous 1 M

(cc) BY

H_2SO_4 electrolyte. To the best of our knowledge, dual or even triple heteroatom doping treatments have been employed to improve the ORR catalytic performance of carbon-based nanostructures [37,38]. Y. Zheng and colleagues [39] used a simple and straightforward template-free technique to fabricate nitrogen/sulfur dual-doped hollow mesoporous carbon nanospheres for ORR electrocatalysis. The unique hollow spherical and mesoporous structure formed in situ from an intricately engineered covalent triazine framework via a thermally initiated hollowing pathway. The material that resulted exhibited high N and S contents, large specific surface areas, and excellent electrochemical performance [39].

Generally speaking, carbon materials have been designed for effective energy conversion and storage due to their unique physicochemical properties, such as high electronic conductivity, large surface area, and adjustable porous structure [22]. In this direction, CNTs have sparked considerable interest in the fields of electrocatalysis, biosensors, and energy storage due to their amazing features, which include exceptional electronic conductivity, great thermal stability, and good mechanical characteristics [40]. Herein, CNTs, l-cysteine (L-Cys), and thiourea (TU) were utilized for dual-doping with a hydrothermal treatment for electrocatalysis. Although N and S dual-doped CNTs have been extensively studied, little attention has been paid to the study of CNTs treated with amino acids-co-thiourea for electrochemical catalysis. Therefore, we investigated the structural change caused by inserting dual heteroatoms into the surface of CNTs, as well as the electrochemical performance in terms of the ORR. For comparison, investigated heteroatom doping of oxidized CNTs to test the hypothesis that heteroatom-doped CNT catalysts functionalized with selective oxygenic groups (COOH or OH) can improve intrinsic reactivity. Neat CNTs, doped CNT prepared at 4 h, and doped (CNT and oxidized CNTs (OCNTs)) prepared at 16 h are denoted as CNT0, D-CNT1, D-CNT2, and D-CNT3, respectively.

Experimental

Materials

Multiwall carbon nanotubes (MWCNTs, ≥98 % purity) were provided by Sigma Aldrich. L-Cys (≥99 % purity) was purchased from Beijing Solarbio Science & Technology. Thiourea (>98 % purity), N, N-Dimethyleformamide DMF, $NaNO_3$ (>98 % purity), and H_2SO_4 (98 %) were supplied by R&M Chemicals. $KMNO_4$ (>99 % purity) and hydrogen peroxide were provided by Chemiz Sdn. Bhd., and Bendosen Laboratory Chemicals, respectively.

Oxidation of CNTs

Typically, 0.1 g of CNTs with 0.1 g of $NaNO_3$ were dispersed in 60 ml H_2SO_4 (78 %) and placed in the sonicated for around 40 minutes at 11 °C in an ice bath, after which 0.2 g of $KMNO_4$ was added to the dispersion portion wise and sonicated for 2 h at (35 to 45 °C). Then 20 ml of 30 wt.% H_2O_2 was progressively added, followed by 300 ml of deionized water. Finally, the CNTs were filtered, washed, and dried.

Hydrothermal synthesis

Typically, 0.2 g of CNTs were dispersed in 100 ml deionized water before being placed in an ultrasonic bath for 2 h at room temperature (Solution A). Then after, 0.15 g of L-Sys and T-U (weight ratio 2:1) was added to 30 ml of solution A and then sonicated for 30 min (Solution B). Solution B was placed into a Teflon-autoclave reactor for hydrothermal reaction and in an oven for the

appropriate reaction time at 160 °C. The reactor was then allowed to cool naturally before the CNTs were filtered, washed, and freeze-dried. The same method was used to treat the oxidized CNTs.

Measurements

X-ray diffractometer (XRD) (D2 PHASER – Bruker, Germany)was used to measure phase patterns of D-CNTs. Cu Kα radiation, Cu anode, and a scanning rate of 10° min^{-1} were used for measurements. Raman spectroscopy (Renishaw inVia, Germany) was used to identify the final chemical structure of modified CNTs.

To further reveal the chemical structure, a Fourier transfer infrared (FTIR) spectrometer (Nicolet iS50 FT-IR, USA) was used to characterize the functional group attached to doped CNTs. Analyses were performed by using the ATR method over a spectral range of 4000 to 500 cm^{-1}. Differential scanning calorimetry (DSC) analysis was performed by using a high-temperature DSC (METTLER TOLEDO, Switzerland) instrument. About 0.5 mg of each sample was heated in an aluminum crucible with a heating rate of 10 °C min^{-1} from 30 to 450 °C.

The morphology and EDS elemental analysis of doped-CNTs were studied using scanning electron microscopy (SEM, JSM-5600LV, Japan). Thermo Scientific elemental analyzer (Flash smart CHNS, Italy) was employed to measure the element content inserted in the modified CNTs. About 3 mg of dried samples were used and the atomic percentage of nitrogen, carbon, hydrogen, and sulfur were determined. ORR of modified samples was carried out on a potentiostat (Auto-Lab PGSTAT302N, Netherlands).

Results and discussion

XRD phase evaluation

XRD patterns for nitrogen-co-sulfur-doped CNTs are shown in Figure 1. The XRD patterns show major peaks at around $2\theta \approx 25$ and 42°. These peaks are assigned to the hexagonal graphite structures (0 0 2) and (1 0 0), respectively [41]. Obviously, when compared to untreated samples, the intensity of reflection of all doped CNTs decreased, which may be attributable to the insertion of doping elements such as N and S. The substitution of a heteroatom (N or S) in the CNTs generates defect sites and disrupts the carbon lattice; these findings demonstrated their less crystalline nature [42]. The Raman spectra support this result, as seen in Figure 2.

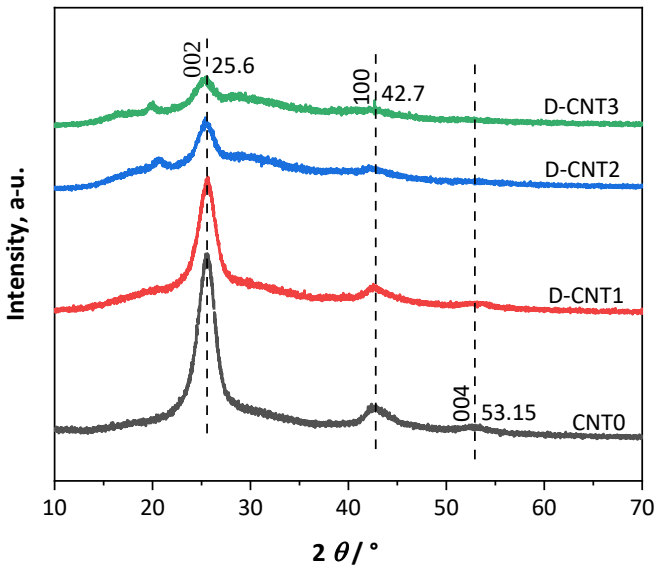

CC BY

***Figure 1**. XRD pattern for the sample of (a) Neat CNTs, (b) D-CNT1, (c) D-CNT2, (d) D-CNT3.*

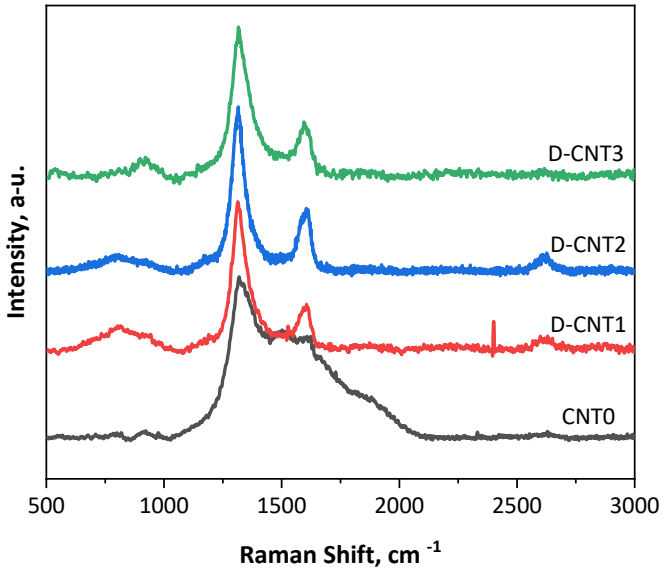

***Figure 2.** Raman spectra for the sample of (a) Neat CNTs, (b) D-CNT1, (c) D-CNT2, (d) D-CNT3*

In particular, D-CNT2 and D-CNT3 exhibited lower intensity for both diffraction peaks than D-CNT1, which could be attributable to a longer doping time. Furthermore, the (100) graphitic plane diffraction peak appears to have vanished in sample D-CNT3, possibly because oxidizing CNTs provided more sites for chemical reactions. CNTs can, in fact, be functionalized in an oxidative environment, therefore CNTs with OH, =CO, O, COOH functionalization are more effective for subsequent reactions [43].

Raman spectroscopy analysis

Raman spectroscopy was used to explore further the sulfur-co-Nitrogen functionalization of CNTs (Figure 3). Two distinct peaks centered at 1350 and 1580 cm^{-1} are identified, corresponding to the disordered carbon (D-band) and the ordered graphitic carbon (G-band). The presence of a D-band with a high intensity indicates the existence of several defects and non-graphitic carbon in the doped CNTs sample, which may have resulted from heteroatoms doping [44]. As can be seen, sample D-CNT2 seems to have the maximum intensity when compared to the other samples. Furthermore, as shown in Figure S1, a corresponding endothermic peak on the DSC curve was identified, which is associated with the degradation/decomposition of the carbon framework. When compared to doped CNT, neat CNT has a lower decomposition temperature. The heat of the reaction rises when doping elements are introduced. These results can be a sign of interaction between CNT and heteroatoms.

Some time ago, it was pointed out that doping with heteroatoms can create chemically active regions, which can boost electrocatalytic activity [44]. The G-band of D-CNT1, DCNT2, and D-CNT3 is obviously shifted to a lower frequency by about 10 cm^{-1}. In the literature, we observed a similar redshift behavior in sulfur-doped carbon nanotubes, indicating the electron delocalization effect caused by π-π interactions between the electron-donor doping precursors and CNT [35]. Overall, the XRD and Raman spectroscopy results suggest the nanocomposite is doped with N and S successfully by our one-step hydrothermal method and that variable doping levels are realized by varying the doping time [45]. In addition, clear evidence and additional conformation of nitrogen and sulfur incorporated into carbon nanotubes are provided in Figure S2.

Furthermore, the D/G peak intensity ratios (I_D/I_G) of D-CNT1, D-CNT2, and D-CNT3 are 1.75, 1.43, and 1.30, respectively. Due to the fact that doping precursors wrapped around the surface of CNTs and covered the partial defect sites, the I_D/I_G ratio was slightly reduced [35].

SEM morphological observation

Figures 3 show SEM images of doped-CNTs. As can be observed, D-CNT2 and D-CNT3 samples contain more clearly irregular nanoparticles, Figure 3b and 3c. This finding indicated their porous nature and high surface area [41]. Several corners and edges are visible on the surfaces of D-CNT2 and D-CNT3, which could become active sites of oxygen adsorption in the ORR process. D-CNT2 has a significant number of pores in its morphology and appears to have a considerably looser porous structure, which helps to improve its ORR activity [46]. To the best of our knowledge, the presence of porous carbons, which give an enhanced accessible surface area for electrolyte ions, is principally responsible for the improved performance of the working electrode [44]. Furthermore, in samples D-CNT2 and D-CNT3, the particles appear densely stacked and agglomerated, implying that agglomeration occurred when amino acids were employed [22,47]. The overlapping and agglomeration behavior leads to forming complex three-dimensional stacked structures [34].

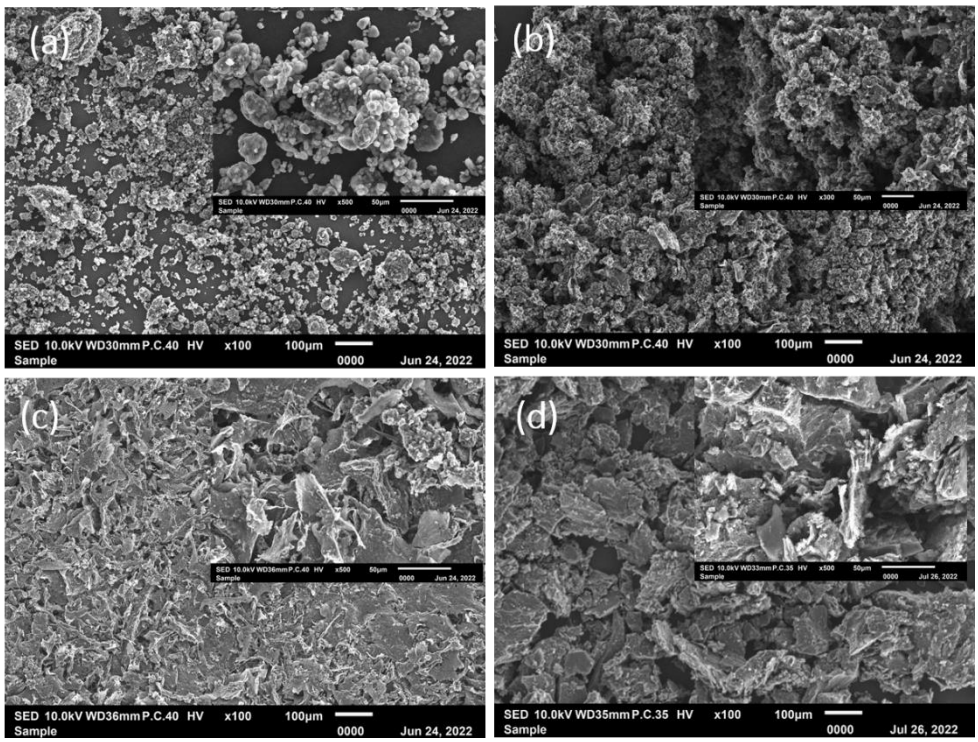

Figure 3 *– SEM images with different magnifications of (a) Neat CNTs, (b) D-CNT1, (c) D-CNT2, (d) D-CNT3*

Elemental analysis

The data from the (CHNS) analysis are shown in Table 1 to confirm the incorporation of doping elements into CNTs' surface. As we can see, The D-CNT3 sample has a slightly lower C content than the other samples, but it has the highest N and S content of 9.38 and 15.20 %, respectively. This is most likely because of the significant doping amount of N and S atoms caused by oxidation of the CNT prior to the doping process, which is consistent with the XRD results. The result of EDS color mapping (Figure S3) further describes the heteroatoms doping of CNTs. As seen the D-CNT3 has a higher S content than D-CNT2. Nitrogen is not detected by SEM-EDX, presumably because nitrogen has a very faint response, making detection unreliable for most materials [48]. Furthermore, EDS may detect major elements with concentrations greater than 10 wt.% [49].

(cc) BY

***Table 1**. Elemental content for the doped sample.*

Sample	Content, wt.%			
	Nitrogen	Carbon	Hydrogen	Sulfur
CNT0	0	88.41	0.102	0.105
D-CNT1	0.572	77.11	0.893	2.744
D-CNT2	1.428	75.695	4.722	5.389
D-CNT3	9.378	41.167	1.872	15.203

Cyclic voltammetry – CV test

The catalytic activity for oxygen reduction reaction of the doped CNTs was measured using cyclic voltammetry (CV) with a three-electrode system (working electrode, counter electrode, and reference electrode) in 1.0 M KOH aqueous electrolyte with potential between − 0.6 and 0.1 V at a scanning rate of 1 and 10 mV s^{-1}. The working electrode was prepared without the addition of any binding materials. The following procedure was used to prepare all working electrodes; 4 mg of D-CNTs were dispersed in 500 µL Alcohol and sonicated for 30 minutes. 1 to 2 µL of dispersion was loaded to the electrode's surface and dried.

Typical cyclic voltammogram curves of doped CNTs cathode/catalyst for the first two or three cycles are displayed in Figure 4. On the CV curves of the D-CNT2 and D-CNT3 samples, a significant ORR peak was observed. D-CNT2 and D-CNT3 have ORR onset potentials of −0.30 and −0.37 V, respectively, while the reduction (cathodic) peaks are at −0.26 and −0.35 V, respectively. The reduction peak of DCNT2 and DCNT3 marginally changed to −0.24 and −0.39 V, respectively, when the scanning rate was increased to 10 mV s^{-1}. These findings demonstrated that D-CNT2 catalysts have stronger ORR catalytic performance than D-CNT3 catalysts. Furthermore, the higher onset potential of D-CNT2 than D-CNT3 implies that the ORR occurs more easily on its surface [34].

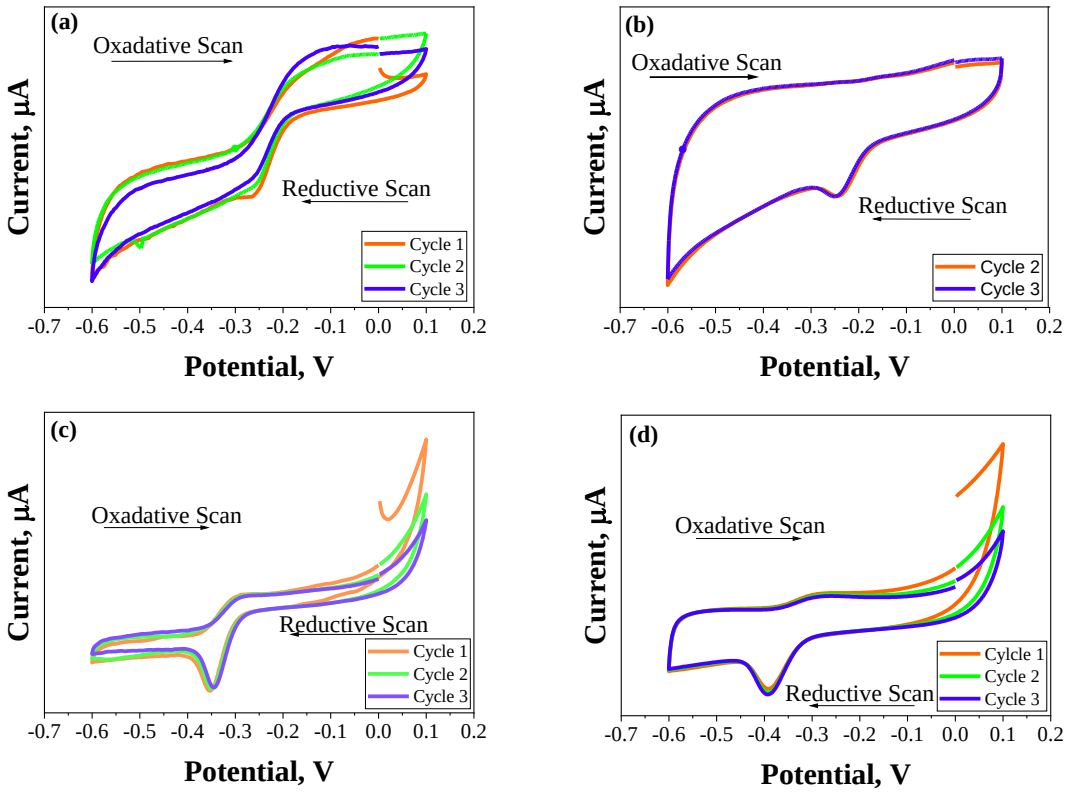

***Figure 4**. Cyclic voltammogram variation of specific capacitance with altering scan rates of the proposed catalysts (a) D-CNT2, scan rate 1 mV s^{-1}; (b) (D-CNT2, scan rate 10 mV s^{-1}; (c) D-CNT3, scan rate 1 mV s^{-1}; (d) D-CNT3, scan rate 0.010 V s^{-1}*

Because of the large number of holes and edges, the DCNT2 electrode has increased activity and a positively shifted onset potential compared to the DCNT3 electrode [50]. To our knowledge, doping with heteroatom can improve the electron-transfer kinetics and consequently the catalytic activity [34]. Besides, Due to a unique electron distribution, the synergistic effect of dual-doping with two dopant elements of different electro-negativities can enhance catalytic activity [51].

Although D-CNT3 contains more N and S than D-CNT2, the latter demonstrated higher ORR catalytic activity, which could be attributed to oxygen-containing functional groups being primarily eliminated below 400 °C [34]. As a result, the reduced oxygen functional group of D-CNT3 during the hydrothermal reaction slightly inhibits ORR activity. According to the Raman analysis, another impact could be the wrapping of doping precursors on the surface of OCNTs and the coverage of partial defect sites.

Additionally, because heteroatom doping can alter surface activity via conjugation between a lone pair of electrons and the π-system of the carbon lattice, it has the potential to generate further pseudo-capacitance improved electrocatalytic activity [22]. Using the CV data, the following equation was used to calculate the variation of specific capacitance with changing scan rates [52]:

$$C_{\mathrm{p}} = \frac{A}{2mk(E_2 - E_1)} \tag{1}$$

where; A is the CV loop's enclosed area and m is the mass of material at the working electrode, k is the scanning rate, and ($E_2 - E_1$) is the potential window (*i.e.,* the entire voltage range through which the electrode system was tested for electrochemical behavior). Table 2 compares the specific capacitance of each doped sample. As shown, C_{p} is noticeably higher when the scanning rate is low (1 mV s^{-1}) and higher in D-CNT2 samples than in D-CNT3 samples, reflecting their effective porosity. To the best of our knowledge, determining specific capacitance at differing scan rates is an essential step in understanding the inherent properties of any electrode material, particularly porosity influences ionic diffusion [52]. The analysis suggests that the dual-doped CNT can be used as an electrocatalyst, and D-CNT2 appears more capacitive than the other sample.

Table 2. *Specific capacity C_p for two differing scanning rates*

Dual–doped samples	Scan rate, mV s^{-1}	Specific capacity, F g^{-1}
D-CNT2	1	214.12
	10	91.14
D-CNT3	1	197.70
	10	124.18

Conclusions

The nitrogen and sulfur dual-doped carbon materials were successfully synthesized with various morphological aspects through a hydrothermal method using l-cysteine and thiourea as precursors. After freeze drying, the resulting D-CNT2 and D-CNT3 exhibited a porous structure. The examination of elemental content proved the existence of sulfur and nitrogen functional groups in CNTs after dual heteroatoms doping. The finding of the electrochemical characterization of the proposed catalysts demonstrates the great ORR activity, which can be attributed to the synergistic effect of dual-doping with dopant elements of different electro-negativities, in addition to the presence of numerous active sites and effective porosity. Besides, heteroatom doping generated the electro-chemical capacitance characteristics. The proposed D-CNT2 catalyst achieved stronger ORR catalytic performance and higher specific capacitance at a lower scanning rate than D-CNT3 catalysts.

(cc) BY

Acknowledgements: *The authors gratefully acknowledge the support and funding provided by the postdoctoral scholarship research program of the Islamic Development Bank (IsDB), KSA (Grant No. 600040856) and the project of Prof. Md Zahangir Alam, Kulliyyah of Engineering, (IIUM) (Grant No. RC-RIGS20-004-0004).*

References

[1] A. Hojjati-Najafabadi, M. Mansoorianfar, T. Liang, K. Shahin, H. Karimi-Maleh, A review on magnetic sensors for monitoring of hazardous pollutants in water resources, *Science of the Total Environment* **824** (2022) 153844. https://doi.org/10.1016/j.scitotenv.2022.153844

[2] C. Karaman, O. Karaman, P.-L. Show, Y. Orooji, H. Karimi-Maleh, Utilization of a double-cross-linked amino-functionalized three-dimensional graphene networks as a monolithic adsorbent for methyl orange removal: equilibrium, kinetics, thermodynamics and artificial neural network modeling, *Environmental Research* **207** (2022) 112156. https://doi.org/10.1016/j.envres.2021.112156

[3] Y. Orooji, B. Tanhaei, A. Ayati, S. H. Tabrizi, M. Alizadeh, F. F. Bamoharram, F. Karimi, S. Salmanpour, J. Rouhi, S. Afshar, Heterogeneous UV-Switchable Au nanoparticles decorated tungstophosphoric acid/TiO2 for efficient photocatalytic degradation process, *Chemosphere* **281** (2021) 130795. https://doi.org/10.1016/j.chemosphere.2021.130795

[4] W. Fan, Y. Hao, An empirical research on the relationship amongst renewable energy consumption, economic growth and foreign direct investment in China, *Renewable Energy* **146** (2020) 598-609. https://doi.org/10.1016/j.renene.2019.06.170

[5] W. S. Ebhota, T.-C. Jen, Fossil fuels environmental challenges and the role of solar photovoltaic technology advances in fast tracking hybrid renewable energy system, *International Journal of Precision Engineering and Manufacturing-Green Technology* **7** (2020) 97-117. https://doi.org/10.1007/s40684-019-00101-9

[6] R. Kumar, A. Pérez del Pino, S. Sahoo, R. K. Singh, W. K. Tan, K. K. Kar, A. Matsuda, E. Joanni, Laser processing of graphene and related materials for energy storage: State of the art and future prospects, *Progress in Energy and Combustion Science* **91** (2022) 100981. https://doi.org/10.1016/j.pecs.2021.100981

[7] A. Aygun, F. Gulbagca, E. E. Altuner, M. Bekmezci, T. Gur, H. Karimi-Maleh, F. Karimi, Y. Vasseghian, F. Sen, Highly active PdPt bimetallic nanoparticles synthesized by one-step bioreduction method: Characterizations, anticancer, antibacterial activities and evaluation of their catalytic effect for hydrogen generation, *International Journal of Hydrogen Energy* **48** (2023) 6666-6679. https://doi.org/10.1016/j.ijhydene.2021.12.144

[8] W. Nimir, A. Al-Othman, M. Tawalbeh, A. Al Makky, A. Ali, H. Karimi-Maleh, F. Karimi, C. Karaman, Approaches towards the development of heteropolyacid-based high temperature membranes for PEM fuel cells, *International Journal of Hydrogen Energy* **48** (2023) 6638-6656. https://doi.org/10.1016/j.ijhydene.2021.11.174

[9] H. Karimi-Maleh, C. Karaman, O. Karaman, F. Karimi, Y. Vasseghian, L. Fu, M. Baghayeri, J. Rouhi, P. Senthil Kumar, P.-L. Show, Nanochemistry approach for the fabrication of Fe and N co-decorated biomass-derived activated carbon frameworks: a promising oxygen reduction reaction electrocatalyst in neutral media, *Journal of Nanostructure in Chemistry* **12** (2022) 429-439. https://doi.org/10.1007/s40097-022-00492-3

[10] X. Wu, J. Jiang, C. Wang, J. Liu, Y. Pu, A. Ragauskas, S. Li, B. Yang, Lignin-derived electrochemical energy materials and systems, Biofuels, *Bioproducts and Biorefining* **14** (2020) 650-672. https://doi.org/10.1002/bbb.2083

[11] H. Kim, J. C. Kim, M. Bianchini, D.-H. Seo, J. Rodriguez-Garcia, G. Ceder, Recent Progress and Perspective in Electrode Materials for K-Ion Batteries, *Advanced Energy Materials* **8** (2018) 1702384. https://doi.org/10.1002/aenm.201702384

[12] A. G. Olabi, Q. Abbas, A. Al Makky, M. A. Abdelkareem, Supercapacitors as next generation energy storage devices: Properties and applications, *Energy* **248** (2022) 123617. https://doi.org/10.1016/j.energy.2022.123617

[13] X. Li, J. Zhou, J. Zhang, M. Li, X. Bi, T. Liu, T. He, J. Cheng, F. Zhang, Y. Li, X. Mu, J. Lu, B. Wang, Bamboo-Like Nitrogen-Doped Carbon Nanotube Forests as Durable Metal-Free Catalysts for Self-Powered Flexible Li–CO2 Batteries, *Advanced Materials* **31** (2019) 1903852. https://doi.org/10.1002/adma.201903852

[14] Z. Peng, Y. Zou, S. Xu, W. Zhong, W. Yang, High-Performance Biomass-Based Flexible Solid-State Supercapacitor Constructed of Pressure-Sensitive Lignin-Based and Cellulose Hydrogels, *ACS Applied Materials & Interfaces* **10** (2018) 22190-22200. https://doi.org/10.1021/acsami.8b05171

[15] W. Cai, X. Tong, X. Yan, H. Li, Y. Li, X. Gao, Y. Guo, W. Wu, D. Fu, X. Huang, J. Liu, H. Wang, Direct carbon solid oxide fuel cells powered by rice husk biochar, *International Journal of Energy Research* **46** (2022) 4965-4974. https://doi.org/10.1002/er.7489

[16] B. He, Q. Zhang, Z. Pan, L. Li, C. Li, Y. Ling, Z. Wang, M. Chen, Z. Wang, Y. Yao, Q. Li, L. Sun, J. Wang, L. Wei, Freestanding Metal–Organic Frameworks and Their Derivatives: An Emerging Platform for Electrochemical Energy Storage and Conversion, *Chemical Reviews* **122** (2022) 10087-10125. https://doi.org/10.1021/acs.chemrev.1c00978

[17] N. Roy, S. Yasmin, A. Ejaz, H.S. Han, S. Jeon, Influence of pyrrolic and pyridinic-N in the size and distribution behaviour of Pd nanoparticles and ORR mechanism, *Applied Surface Science* **533** (2020) 147500. https://doi.org/10.1016/j.apsusc.2020.147500

[18] I. Baskin, Y. Ein-Eli, Electrochemoinformatics as an Emerging Scientific Field for Designing Materials and Electrochemical Energy Storage and Conversion Devices—An Application in Battery Science and Technology, *Advanced Energy Materials* **12** (2022) 2202380. https://doi.org/10.1002/aenm.202202380

[19] J. Wang, C.-X. Zhao, J.-N. Liu, D. Ren, B.-Q. Li, J.-Q. Huang, Q. Zhang, Quantitative kinetic analysis on oxygen reduction reaction: A perspective, *Nano Materials Science* **3** (2021) 313-318. https://doi.org/10.1016/j.nanoms.2021.03.006

[20] X. Yu, Y. Ma, C. Li, X. Guan, Q. Fang, S. Qiu, A Nitrogen, Sulfur co-Doped Porphyrin-based Covalent Organic Framework as an Efficient Catalyst for Oxygen Reduction, *Chemical Research in Chinese Universities* **38** (2022) 167-172. https://doi.org/10.1007/s40242-021-1374-1

[21] S. Shi, Y. Wang, B. Wang, F. Wu, Y. Suo, Z. Zhang, Y. Xu, Cobalt, sulfur, nitrogen co-doped carbon as highly active electrocatalysts towards oxygen reduction reaction, International *Journal of Hydrogen Energy* **47** (2022) 39058-39069. https://doi.org/10.1016/j.ijhydene.2022.09.073

[22] D. Wu, T. Wang, L. Wang, D. Jia, Hydrothermal synthesis of nitrogen, sulfur co-doped graphene and its high performance in supercapacitor and oxygen reduction reaction, *Microporous and Mesoporous Materials* **290** (2019) 109556. https://doi.org/10.1016/j.micromeso.2019.06.018

[23] G. Rambabu, Z. Turtayeva, F. Xu, G. Maranzana, M. Emo, S. Hupont, M. Mamlouk, A. Desforges, B. Vigolo, Insights into the electrocatalytic behavior of nitrogen and sulfur co-doped carbon nanotubes toward oxygen reduction reaction in alkaline media, *Journal of Materials Science* **57** (2022) 16739-16754. https://doi.org/10.1007/s10853-022-07653-3

[24] D. Yan, Y. Han, Z. Ma, Q. Wang, X. Wang, Y. Li, G. Sun, Magnesium lignosulfonate-derived N, S co-doped 3D flower-like hierarchically porous carbon as an advanced metal-free electrocatalyst towards oxygen reduction reaction, *International Journal of Biological Macromolecules* **209** (2022) 904-911. https://doi.org/10.1016/j.ijbiomac.2022.04.063

(cc) BY

[25] Z. Chen, D. Higgins, A. Yu, L. Zhang, J. Zhang, A review on non-precious metal electrocatalysts for PEM fuel cells, *Energy & Environmental Science* **4** (2011) 3167-3192. https://doi.org/10.1039/C0EE00558D

[26] M. Zhang, L. Dai, Carbon nanomaterials as metal-free catalysts in next generation fuel cells, *Nano Energy* **1** (2012) 514-517. https://doi.org/10.1016/j.nanoen.2012.02.008

[27] W. Wong, W. Daud, A. Mohamad, A. Kadhum, K. Loh, E. Majlan, Recent progress in nitrogen-doped carbon and its composites as electrocatalysts for fuel cell applications, *International Journal of Hydrogen Energy* **38** (2013) 9370-9386. https://doi.org/10.1016/j.ijhydene.2012.12.095

[28] Y. Jiao, Y. Zheng, K. Davey, S.-Z. Qiao, Activity origin and catalyst design principles for electrocatalytic hydrogen evolution on heteroatom-doped graphene, *Nature Energy* **1** (2016) 16130. https://doi.org/10.1038/nenergy.2016.130

[29] J.H. Kim, Y.-i. Ko, Y.A. Kim, K.S. Kim, C.-M. Yang, Sulfur-doped carbon nanotubes as a conducting agent in supercapacitor electrodes, *Journal of Alloys and Compounds* **855** (2021) 157282. https://doi.org/10.1016/j.jallcom.2020.157282

[30] W.-L. Xin, L.-H. Xu, K.-K. Lu, D. Shan, Boosting oxygen reduction catalysis with Fe-N@ ZnO codoped highly graphitized carbon derived from N, N'-carbonyldiimidazole-Induced bimetallic coordinated polymer, *Applied Surface Science* **505** (2020) 144605. https://doi.org/10.1016/j.apsusc.2019.144605

[31] X. Qiu, Y. Yu, Z. Peng, M. Asif, Z. Wang, L. Jiang, W. Wang, Z. Xu, H. Wang, H. Liu, Cobalt sulfides nanoparticles encapsulated in N, S co-doped carbon substrate for highly efficient oxygen reduction, *Journal of Alloys and Compounds* **815** (2020) 152457. https://doi.org/10.1016/j.jallcom.2019.152457

[32] D.-W. Wang, D. Su, Heterogeneous nanocarbon materials for oxygen reduction reaction, *Energy & Environmental Science* **7** (2014) 576-591. https://doi.org/10.1039/C3EE43463J

[33] R. Atchudan, T. N. J. I. Edison, S. Perumal, A. S. Parveen, Y. R. Lee, Electrocatalytic and energy storage performance of bio-derived sulphur-nitrogen-doped carbon, *Journal of Electroanalytical Chemistry* **833** (2019) 357-369. https://doi.org/10.1016/j.jelechem.2018.12.007

[34] X. Xu, T. Yuan, Y. Zhou, Y. Li, J. Lu, X. Tian, D. Wang, J. Wang, Facile synthesis of boron and nitrogen-doped graphene as efficient electrocatalyst for the oxygen reduction reaction in alkaline media, *International Journal of Hydrogen Energy* **39** (2014) 16043-16052. https://doi.org/10.1016/j.ijhydene.2013.12.079

[35] J.-J. Fan, Y.-J. Fan, R.-X. Wang, S. Xiang, H.-G. Tang, S.-G. Sun, A novel strategy for the synthesis of sulfur-doped carbon nanotubes as a highly efficient Pt catalyst support toward the methanol oxidation reaction, *Journal of Materials Chemistry* A **5** (2017) 19467-19475. https://doi.org/10.1039/C7TA05102F

[36] R. Atchudan, T.N . Jebakumar Immanuel Edison, S. Perumal, R. Vinodh, R. S. Babu, A. K. Sundramoorthy, A. A. Renita, Y. R. Lee, Facile synthesis of nitrogen-doped porous carbon materials using waste biomass for energy storage applications, *Chemosphere* **289** (2022) 133225. https://doi.org/10.1016/j.chemosphere.2021.133225

[37] Y. Shen, Y. Li, G. Yang, Q. Zhang, H. Liang, F. Peng, Lignin derived multi-doped (N, S, Cl) carbon materials as excellent electrocatalyst for oxygen reduction reaction in proton exchange membrane fuel cells, *Journal of Energy Chemistry* **44** (2020) 106-114. https://doi.org/10.1016/j.jechem.2019.09.019

[38] Z. Lu, Z. Li, S. Huang, J. Wang, R. Qi, H. Zhao, Q. Wang, Y. Zhao, Construction of 3D carbon network with N, B, F-tridoping for efficient oxygen reduction reaction electrocatalysis and high performance zinc air battery, *Applied Surface Science* **507** (2020) 145154. https://doi.org/10.1016/j.apsusc.2019.145154

[39] Y. Zheng, S. Chen, K. A. I. Zhang, J. Guan, X. Yu, W. Peng, H. Song, J. Zhu, J. Xu, X. Fan, C. Zhang, T. Liu, Template-free construction of hollow mesoporous carbon spheres from a covalent triazine framework for enhanced oxygen electroreduction, *Journal of Colloid and Interface Science* **608** (2021) 3168-3177. https://doi.org/10.1016/j.jcis.2021.11.048

[40] J. Wang, X. Yan, Z. Zhang, H. Ying, R. Guo, W. Yang, W.Q. Han, Facile preparation of high-content N-doped CNT microspheres for high-performance lithium storage, *Advanced Functional Materials* **29** (2019) 1904819. https://doi.org/10.1002/adfm.201904819

[41] A. Osikoya, D. Wankasi, R. Vala, C. Dikio, A. Afolabi, N. Ayawei, E. Dikio, Synthesis, characterization and sorption studies of nitrogen–doped carbon nanotubes, *Digest Journal of Nanomaterials and Biostructures* **10** (2015) 125-134.

[42] A. Ariharan, B. Viswanathan, V. Nandhakumar, Nitrogen-incorporated carbon nanotube derived from polystyrene and polypyrrole as hydrogen storage material, *International Journal of Hydrogen Energy* **43** (2018) 5077-5088. https://doi.org/10.1016/j.ijhydene.2018.01.110

[43] J. Wei, R. Lv, N. Guo, H. Wang, X. Bai, A. Mathkar, F. Kang, H. Zhu, K. Wang, D. Wu, Preparation of highly oxidized nitrogen-doped carbon nanotubes, *Nanotechnology* **23** (2012) 155601. https://doi.org/10.1088/0957-4484/23/15/155601

[44] G. Sun, H. Xie, J. Ran, L. Ma, X. Shen, J. Hu, H. Tong, Rational design of uniformly embedded metal oxide nanoparticles into nitrogen-doped carbon aerogel for high-performance asymmetric supercapacitors with a high operating voltage window, *Journal of Materials Chemistry A* **4** (2016) 16576-16587. https://doi.org/10.1039/C6TA07240B

[45] J. Zhao, Y. Liu, X. Quan, S. Chen, H. Zhao, H. Yu, Nitrogen and sulfur co-doped graphene/carbon nanotube as metal-free electrocatalyst for oxygen evolution reaction: the enhanced performance by sulfur doping, *Electrochimica Acta* **204** (2016) 169-175. https://doi.org/10.1016/j.electacta.2016.04.034

[46] J. Guo, S. Zhang, M. Zheng, J. Tang, L. Liu, J. Chen, X. Wang, Graphitic-N-rich N-doped graphene as a high performance catalyst for oxygen reduction reaction in alkaline solution, *International Journal of Hydrogen Energy* **45** (2020) 32402-32412. https://doi.org/10.1016/j.ijhydene.2020.08.210

[47] T. Wang, L. Wang, D. Wu, W. Xia, H. Zhao, D. Jia, Hydrothermal synthesis of nitrogen-doped graphene hydrogels using amino acids with different acidities as doping agents, *Journal of Materials Chemistry A* **2** (2014) 8352-8361. https://doi.org/10.1039/C4TA00170B

[48] W. J. Wolfgong, *Chemical analysis techniques for failure analysis: Common instrumental methods*, in *Handbook of Materials Failure Analysis with Case Studies from the Aerospace and Automotive Industries* ,A. S. H. Makhlouf, M. Aliofkhazraei, Eds., Butterworth-Heinemann, Boston, USA, 2016 pp. 279-307. https://doi.org/10.1016/B978-0-12-800950-5.00014-4

[49] S. Nasrazadani, S. Hassani, *Modern analytical techniques in failure analysis of aerospace, chemical, and oil and gas industries*, in *Handbook of Materials Failure Analysis with Case Studies from the Oil and Gas Industry*, A. S. H. Makhlouf, M. Aliofkhazraei, Eds., Butterworth-Heinemann, Boston, USA, 2016 pp. 39-54. https://doi.org/10.1016/B978-0-08-100117-2.00010-8

[50] K. Kakaei, G. Ghadimi, A green method for Nitrogen-doped graphene and its application for oxygen reduction reaction in alkaline media, *Materials Technology* **36** (2021) 46-53. https://doi.org/10.1080/10667857.2020.1724692

[51] H. Liu, P. Sun, M. Feng, H. Liu, S. Yang, L. Wang, Z. Wang, Nitrogen and sulfur co-doped CNT-COOH as an efficient metal-free catalyst for the degradation of UV filter BP-4 based on sulfate radicals, *Applied Catalysis B: Environmental* **187** (2016) 1-10. https://doi.org/10.1016/j.apcatb.2016.01.036

(cc) BY

[52] H. Siraj, K. S. Ahmad, S. B. Jaffri, M. Sohail, Synthesis, characterization and electrochemical investigation of physical vapor deposited barium sulphide doped iron sulphide dithiocarbamate thin films, *Microelectronic Engineering* **233** (2020) 111400. https://doi.org/10.1016/j.mee.2020.111400

©2023 by the authors; licensee IAPC, Zagreb, Croatia. This article is an open-access article distributed under the terms and conditions of the Creative Commons Attribution license (https://creativecommons.org/licenses/by/4.0/)